

Smooth halos in the cosmic web

José Gaite

Physics Dept., ETSIAE, IDR, Universidad Politécnica de Madrid, E-28040 Madrid, Spain

E-mail: jose.gaite@upm.es

Abstract. Dark matter halos can be defined as smooth distributions of dark matter placed in a non-smooth cosmic web structure. This definition of halos demands a precise definition of smoothness and a characterization of the manner in which the transition from smooth halos to the cosmic web takes place. We introduce entropic measures of smoothness, related to measures of inequality previously used in economy and with the advantage of being connected with standard methods of multifractal analysis already used for characterizing the cosmic web structure in cold dark matter N -body simulations. These entropic measures provide us with a quantitative description of the transition from the small scales portrayed as a distribution of halos to the larger scales portrayed as a cosmic web and, therefore, allow us to assign definite sizes to halos. However, these “smoothness sizes” have no direct relation to the virial radii. Finally, we discuss the influence of N -body discreteness parameters on smoothness.

Keywords: cosmic web, cosmological simulations, superclusters

Contents

1	Introduction	2
2	Smoothness and isotropy of halos	4
2.1	Counts in cells for spherical shells	6
2.2	Entropic measures	7
2.3	Graininess versus triaxiality	9
3	Smoothness of halos in N-body simulations	9
3.1	Bolshoi and Via Lactea II simulations	9
3.2	Multifractal analysis of the Bolshoi simulation	10
3.3	Analysis of Bolshoi’s halos	11
3.4	Analysis of the Via Lactea II halo	13
4	N-body discreteness and smoothness of halos	14
5	Summary and conclusions	16
A	Appendix: multifractal analysis	20

1 Introduction

The large scale structure of the Universe can be described as a “cosmic web” formed by matter sheets, filaments, and nodes, plus the cosmic voids that these objects leave in between. This type of structure was initially proposed in connection with simplified but insightful models of the cosmic dynamics, namely, the Zeldovich approximation and the adhesion model [1–4]. It has been since confirmed by galaxy surveys [5–7] and cosmological N -body simulations [8–10]. N -body simulations have especially contributed to the understanding of structure formation. In particular, the analysis of cold dark matter (CDM) N -body simulations has consistently shown that, on smaller scales, the cosmic-web structure transforms into a distribution of relatively smooth dark matter clusters or *halos* that have a limited range of sizes. Halo models of the large scale structure of matter [11] are now very popular indeed. Dark matter halos were initially introduced to model the invisible matter surrounding galaxies, but present halo models are concerned with the large scale distribution of halos in space [12–14] as well as with the distribution of matter within individual halos [15–17]. Actually, the essence of halo models is to separate the full dark matter distribution into one part corresponding to the distribution of dark matter inside halos and another corresponding to the distribution of halo centers in space [11]. The distribution of dark matter inside a halo is smooth, save for the density singularity at its center and the possible presence of other halos (subhalos) close to it. The distribution of halo centers in space must follow the cosmic-web structure.

The geometry of the cosmic-web structure in the adhesion model belongs to the geometric type of mass distributions that have noticeable geometric features on ever decreasing scales. This type of geometry is generally referred to as fractal geometry [18]. Fractal geometry typically appears in nonlinear dynamical systems in which the dynamics is characterized by the absence of reference scales and is driven to an attractor, independent of the initial conditions. The dynamics of collision-less CDM, only ruled by the gravitational interaction, is scale invariant, although the initial conditions are not and it is usually assumed that they determine the geometry in the nonlinear regime. The adhesion model [3, 4] gives rise to a self-similar cosmic web that indeed depends on an initial *power-law* spectrum of fluctuations [19]; but in the *stochastic* adhesion model [20, 21], equivalent to the Kardar-Parisi-Zhang equation of interface growth [22], the cosmic-web is actually an attractor independent of the initial conditions. At any rate, the fractal analysis and, more specifically, the multifractal analysis of the large-scale structure have a long history, including analyses of the distribution of galaxies [23–26] and of CDM N -body simulations [27–33]. Furthermore, the CDM structure produced by N -body simulations can be described as a distribution of halos in a multifractal cosmic structure [30, 31, 34]. Whether or not the cosmic web is self-similar, its multifractal spectrum and, specifically, its Rényi dimensions can be reliably computed in CDM N -body simulations (multifractality does not imply self-similarity) [31, 33]. That is what we need in the present work.

The adhesion model is soluble and produces a distribution of singular sheets, filaments and nodes of vanishing size in the limit of vanishing viscosity [3, 4]. The regularizing effect of a finite viscosity smoothens these structures and gives them a size proportional to it. This suggests that the smoothness of halos in CDM N -body simulations may be influenced by the regularizing effects, on small scales, of N -body discreteness and the associated gravity softening [35]. In other words, the range of halo sizes may depend on the discreteness scales, namely, the discretization length $N^{-1/3}$ (length of the cube with one particle on average), and the gravity-softening length. N -body discreteness primarily affects underdense regions:

the structure of cosmic voids is lost on scales smaller than the discretization length [31, 32]. Therefore, the web structure must undergo a morphological transition on scales of the order of the discretization length, and smaller scales can only provide, at best, a distorted portrait of the cosmic web.

At any rate, halos, as high density regions, are generally well sampled below the discretization length, unlike voids. In fact, the part of the cosmic-web multifractal spectrum that corresponds to high density regions and, consequently, to halos can be obtained accurately on scales considerably smaller than $N^{-1/3}$ [31, 33]. Therefore, one may wonder why the smooth aspect of halos is so different from a cosmic-web structure, that is to say, why such a drastic transformation takes place on scales close to the discretization length. A thorough analysis of the influence of discretization on the sizes and the smoothness of halos would require us to compare various N -body simulations and, therefore, it would demand a considerable use of computing resources. Before undertaking this job, it is necessary to have a better understanding of the factors determining the size and smoothness of halos and the transition to the cosmic web structure in N -body simulations. This can be achieved with the analysis of one N -body simulation with good resolution. We analyze the Bolshoi simulation [36, 37].

Dark matter halos were initially conceived as dark matter concentrations that are approximately spherical and centered on peaks of the density field, although now it is understood that halos are more or less ellipsoidal [11]. Halos are usually bounded at their virial radii, but there is no natural halo boundary and there are various definitions of it [38]. The definition that places the halo boundary at the virial radius can be criticized on various grounds and, especially, concerning the suitability of the spherical collapse model [35]. An alternative is precisely to use smoothness as the property of the dark matter distribution in a halo that defines its boundary. One of the questions we intend to answer is whether the “smoothness” radius is related to the virial radius.

Although smoothness is easily perceived by the human eye, a precise (mathematical) definition of it is not obvious and may depend somewhat on the application. Therefore, our first concern must be to provide a characterization of smoothness that is suitable for N -body simulations. Of course, the smoothness of dark matter halos, or, rather, their non-smoothness, has already been studied in the literature. In fact, one of the central problems of the CDM model, namely, the “missing satellites problem”, is directly related to the graininess of dark matter halos [39]. To quantify the graininess of dark matter halos, Zemp et al [40] employ statistical measures and apply them to a Milky Way-mass dark matter halo in an N -body simulation, namely, the Via Lactea II (VL2) simulation [41]. Our work is related to Zemp et al’s [40], but we consider the question of inner halo structure in relation to the larger scale structure, that is to say, our concern is the transition from a smooth distribution on halo scales to a non-smooth and strongly anisotropic cosmic-web structure on larger scales (or vice versa). Therefore, our statistical methods are essentially different from theirs and actually are an adaptation of multifractal methods to the analysis of individual halos. After developing this method, we can analyze the smoothness of halos in N -body simulations to determine the variation of smoothness with growing halo radius and determine how smoothness disappears and gives way to cosmic-web non-smoothness.

As mentioned above, N -body discreteness effects must play a role in the transition from smooth halos to the cosmic web in CDM simulations. Discreteness effects are due to having N bodies and the related gravity softening. A softening length is needed in every method of gravity softening and is commonly chosen to be much smaller than the discretization length

$N^{-1/3}$ [42]. Whether this is correct or not is a controversial issue [43–46], but it is commonly accepted that it is. We briefly study the influence of the two scales on the size of halos, which is an important but still moot question.

Last, let us mention, as a matter of interest, that some new studies of cosmic structure consider the description of structure in the six-dimensional phase space. Zemp et al [40] already relate graininess of the spatial distribution to features of the velocity field that can be interpreted as the presence of streams of matter. The multi-stream nature of phase space is further studied by Shandarin [47], Abel et al [48] and Neyrinck [49]. Our method for the analysis of smoothness of the distribution in real space can be extended to phase space, but this extension is beyond the scope of the present work.

To summarize, our plan is the following. The problem of halo smoothness is presented in Sect. 2. We introduce an entropic measure of (non)smoothness that is suitable for N -body simulations and constitutes a new method of multifractal analysis of halos. Then, we compare our entropic measure to the measures of Zemp et al (Sects. 2.1 and 2.2). In Sect. 3, we apply our measure to a number of halos from the Bolshoi simulation and to the Milky-Way VL2 halo. The latter is useful for a quantitative comparison with the results of Zemp et al, but the Bolshoi simulation contains a large number of halos which allow us to compare different halos in the same simulation. In addition, the Bolshoi simulation is suitable for a multifractal analysis of the cosmic-web structure (Sect. 3.2) that is useful to characterize the transition from halos to the cosmic web. In Sect. 4, we consider the relation between the smoothness of halos and the discreteness parameters of N -body simulations. We present our conclusions in Sect. 5. Finally, we include appendix A, with basic techniques of multifractal analysis, as applied to N -body simulations.

2 Smoothness and isotropy of halos

A dark matter halo consists of a distribution of dark matter particles with a radial density profile that is singular at the center [11]. In general, this singularity is found to be of power-law type, although its exact form could be slightly more complicated [17]. For $r > 0$, the density is finite and a smooth function of the coordinates. The question addressed in this paper is the extent of the smooth distribution of matter that can be associated with halos rather than the precise properties of the halo radial density profile. The question of smoothness is essentially the same question studied by Zemp et al [40], because graininess is opposite to smoothness, so smoothness ends where graininess begins. Although it may be taken for granted that the distribution of dark matter is smooth on sufficiently small scales, this is not a logical necessity, and in a fully multifractal cosmic web structure the singularities appear everywhere, not only in isolated halo centers [30, 31].

The first problem to characterize the smoothness of halos is that there is no general agreement on how to define individual halos in N -body simulations (for a recent and comprehensive reference about halo finding, see [38]). Nevertheless, halos certainly are mass concentrations, and most halo finders begin by locating peaks in a suitably defined coarse-grained density field, which are the potential halo centers [38]. Of course, there is no unique definition of this coarse-grained density field, so the locations of halo centers may be slightly inaccurate, but this is not important. Once chosen one halo center, it is necessary to determine the extent of the halo. According to our hypothesis, the halo ends where the smooth distribution of particles transforms into a grainy distribution identifiable with the expected large-scale cosmic-web structure. This transformation is obvious as we zoom in or out on

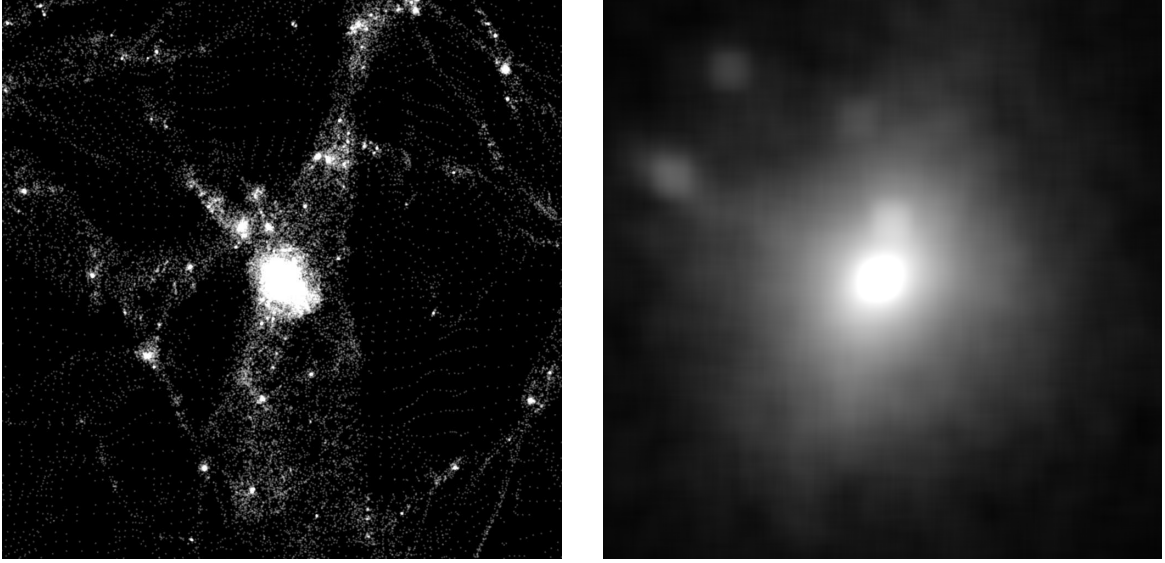


Figure 1. (Left) Cosmic web around a Bolshoi simulation massive halo, at the scale of $15.6 \text{ Mpc}/h$, showing a grainy and filamentary structure. (Right) Close-up on the same halo, spanning $458 \text{ kpc}/h$, showing a smooth and quasi-spherical mass concentration.

any halo, as can be seen in Fig. 1 (where the density field has been obtained by Gaussian filtering with $\sigma = 15 \text{ kpc}/h$).¹ If we imagine a spherical surface with origin on a halo center and with increasing radius, at some radius, that surface must intersect a distribution that is essentially indistinguishable from the cosmic web.

Let us consider the cosmic web produced by the adhesion model, which is calculable and reaches infinitesimally small scales [19]. This cosmic-web structure displays strong anisotropy and a rapid variation of the (coarse-grained) density between neighboring points, unlike a smooth matter distribution. The anisotropy and the rapid variation of density are also perceived in images of N -body simulations, e.g., Fig. 1, left. But we need precise mathematical definitions that allow us to measure them. Mathematically, a function is smooth if it is differentiable. Therefore, the natural procedure to determine the smoothness of a point distribution that results from an N -body simulation should be to compute derivatives of the coarse-grained density. Thus, the first problem would be to define a coarse-grained density and its derivatives. However, there arises a serious problem with this method: one cannot expect smoothness of the small scale dark matter distribution in the mathematical sense, because halo radial density profiles are singular at $r = 0$. At a singular point, the density and its derivatives diverge. Nevertheless, we expect that isolated singularities preserve some degree of smoothness, unlike the singularities in typical multifractals, which make them totally non-smooth. However, we have to bear in mind that a collection of isolated power-law singularities can approach an ordinary multifractal as the density of singular points increases [30], so the difference between a multifractal cosmic web and a suitable distribution of smooth halos with power-law profiles is quantitative rather than qualitative. We can measure the degree of smoothness by comparing global measures of the magnitudes of the derivatives of the coarse-grained density as functions of the coarse-graining length. We have tried this

¹Cosmic web features are clearly visible in the density field, but sharper renderings of them are provided by Abel et al’s visualization method [48], which takes advantage of the full phase space structure.

method but it is rather cumbersome.

At any rate, a more useful feature distinguishing between the dark matter distribution inside halos and the cosmic web is the change from mild to strong anisotropy. A deep study of the cosmic-web anisotropy requires sophisticated mathematical concepts. Indeed, the cosmic-web anisotropy is due to its morphological structure, namely, to its filaments and sheets, which are described through sophisticated topological constructions [50–52]. Whatever the method employed to measure the cosmic-web morphology, we know that the anisotropy, close to a halo center, can be just reduced to an ellipsoidal profile, whereas, on larger scales, the anisotropy patterns are much more complex (Fig. 1). If we consider a spherical shell centered on a halo, the density in it must be fairly smooth for small radius but become increasingly non-smooth as its radius grows. In other words, non-smoothness and anisotropy are closely related. To be precise, the type of anisotropy that is relevant for delimiting a halo is characterized by the degree of non-smoothness inside spherical shells. Therefore, smoothness can be measured through anisotropy and vice versa. Note that the singularity at the halo center is avoided by measuring smoothness only in spherical shells.

Now, we need to devise a measure of non-smoothness of the distribution in a spherical shell. We expect to find a smooth source of anisotropy at all radii, namely, triaxiality, but also sharp local deviations from isotropy due to the presence of subhalos, which must appear at some distance from the center. Farther from the center, there appear more complex patterns, in particular, underdense regions and holes [40], as the shell intersects the voids of the cosmic web structure. In summary, we must expect that the smooth distribution in a small-radius shell transforms, as the radius gets large, into a very inhomogeneous distribution that displays features corresponding to the cosmic web.

2.1 Counts in cells for spherical shells

To measure the non-uniformity of the distribution of particles in a spherical shell, we can compare the angular spherical coordinates of the particles in it, say $\{\phi_i, \theta_i\}_{i=1}^k$, to the ones corresponding to a uniform distribution. To do this, we must realize that, for a uniform distribution in spherical coordinates, the azimuth angle ϕ must have a uniform distribution in $[0, 2\pi]$, but this does not apply to the polar angle θ : actually, it is $\cos\theta$ the quantity that must be uniformly distributed in its range, $[-1, 1]$. For simplicity, we use $\phi/(2\pi)$ and $(1 + \cos\theta)/2$, which must have a uniform density in the unit square $[0, 1] \times [0, 1]$. These coordinates, of course, belong to the set of coordinate systems defined in geography for cylindrical equal-area projections [53] (but note that the square projection is uncommon). To check if the density of the k values of these redefined angular coordinates conforms to uniformity, we can use counts in cells: in a uniform distribution, the fluctuations of counts in cells conform to the binomial distribution or, for sufficiently large samples, to the Poisson distribution.

While it is easy to test for the Poisson distribution, for example, we must take into account that there are two expected sources of non-uniformity, namely, the triaxiality of halos and the presence of subhalos in a given halo. This is pointed out by Zemp et al [40], who propose to evaluate underdense regions in the VL2 halo as a more suitable measure of its graininess. In this regard, one could apply to the study of voids in the distribution of particles in a spherical shell statistical methods similar to the ones applied to voids in the full three-dimensional particle distribution (such as the methods in [32], for example). Zemp et al [40] actually use one elementary statistic: the void probability function, namely, the probability that a *given* region be empty (the region that they take is a small ball with center

in the shell). This statistic is sufficient to rule out (for large enough shell radius) a uniform distribution or even a smooth triaxial distribution with subhalos, as they do.

The void probability function can also be estimated from counts-in-cells in a spherical shell. However, it is useful to consider quantities that are not only concerned with almost empty cells, belonging to voids. In fact, the most useful quantities must take all the cells into account and provide a measure of the inequality or statistical dispersion of counts-in-cells. Such quantities are commonly employed in economy, for example, to measure inequality of income, where the units of income are individuals, cities, etc. [54]. Zemp et al [40] employ the Gini coefficient, one inequality measure that has become very popular. Another inequality measure very popular in economy is Theil’s entropic index [54], which is inspired by information theory. Indeed, the problem of income distribution is just one instance of the general problem of the partition of some measurable quantity (mass, money, etc.). When this quantity is discrete, the partition problem is equivalent to the combinatorial problem of the distribution of a set of particles in a number of cells. The standard measure of uncertainty in the choice of one particle is the Boltzmann-Gibbs-Shannon (BGS) entropy. A useful generalization of it is the Rényi entropy [55], which constitutes a suitable measure of the statistical dispersion of a partition in cells and, as such, can be used in the analysis of cosmological N -body simulations [33]. Here, this dispersion measure is applied to spherical shells of a halo. Let us notice that generalized entropy indices are also employed in economy [54], but they are based on a type of entropy that is different from Rényi entropy and does not have all its desirable properties; in particular, it is not additive.

2.2 Entropic measures

The Rényi entropies

$$S_q(\{p_i\}) = \frac{\log_2(\sum_{i=1}^M p_i^q)}{1-q}, \quad q \neq 1, \quad (2.1)$$

measure the statistical dispersion of counts-in-cells $\{n_i\}_{i=1}^M$, corresponding to the partition of $N = \sum_{i=1}^M n_i$ particles in M cells, in terms of “probabilities” $\{p_i = n_i/N\}_{i=1}^M$. The limit of S_q as $q \rightarrow 1$ just yields the standard BGS entropy. The Rényi entropies with $q \geq 0$ are bound, namely, $0 \leq S_q(\{p_i\}) \leq \log_2 M$. Hence, it is convenient to divide them by $\log_2 M$, so that they become numbers between 0 and 1, the former corresponding to maximum order or inequality, and the latter to minimum order (uniformity). Then, these bounds are the same ones as the bounds of the Gini coefficient, although their meaning is reversed. The entropic coefficients defined in that way, namely, $S_q(\{p_i\})/\log_2 M$, are related to Rényi *dimensions* (see appendix A). Indeed, the entropic coefficients are just coarse Rényi dimensions [56] divided by the dimension of the ambient space, which is, in the present case, a two-dimensional spherical surface, instead of the ordinary three-dimensional Euclidean space. Therefore, we can consider the entropic coefficients alternately as constituting a particular type of inequality measures or as a sort of coarse Rényi dimensions (independent of the dimension of the ambient space).

The connection of entropic coefficients with Rényi dimensions solves the general problem of the dependence of inequality measures on the chosen unit, that is to say, on the size of the cell, in our case. Unlike in economy, where the division of income into individuals or other units is natural, our cell size is arbitrary. However, this arbitrariness is immaterial provided that the coarse Rényi dimensions converge to their values D_q in the continuum limit, namely, in the limit in which the number of particles and the number of cells tend to infinity.

This convergence takes place in multifractals and guarantees certain independence of cell size. Indeed, a multifractal distribution is precisely defined by the existence of the moment exponents $\tau(q) = (q - 1)D_q$. Notice that self-similarity is a sufficient but *not necessary* condition for it. The property of the Rényi entropic coefficients of converging to definite values in the continuum limit is not shared by the Gini coefficient or other inequality measures. The coarse Rényi dimensions of halo shells, in addition to being only mildly dependent on the cell size, are certainly useful to relate individual halos to the full multifractal cosmic-web structure.

Therefore, we employ the entropic coefficients $S_q(\{p_i\})/\log_2 M$ of the counts-in-cells in the unit square corresponding to equal-area angular coordinates of particles in a spherical shell of a halo. Next, we have to determine the thicknesses of shells and the numbers of cells in them. These are related issues: every shell must contain a sufficient number of particles for meaningful counts, that is to say, for not having too small numbers of cells and of particles per cell. A too small number of cells may average out large fluctuations that take place on small scales. Indeed, the entropic coefficients $S_q/\log_2 M$ are certain to approach the Rényi dimensions only for large M . On the other hand, for a given number of particles in one shell, a too large M leaves most cells empty, and the occupied ones can only have too small numbers of particles. Unfortunately, we cannot have a big number of particles per shell, especially, for small radii, because it makes the shell too thick; that is to say, a compromise is needed. We find it suitable to have 1024 particles per shell, for any radius, and $M = 64$ cells per shell, obtained with a 8×8 mesh in the unit square. These 64 cells play the role of the 10^4 spheres used by Zemp et al [40] for the computation of Gini coefficients (and other quantities). Our number of cells is much smaller but is sufficient: we have checked that it does not lead to noticeable statistical errors (for reasonable values of q).

When we observe how the $q \geq 1$ entropic coefficients of a shell in a given halo vary with the radius of the shell, we notice that they start at values close to one and have a generally decreasing trend. This is in accord with the expected transition from small-scale smoothness to large-scale graininess. However, we can also notice that the regular decreasing trend is punctuated by sudden dips, which naturally correspond to strong inhomogeneities due to subhalos. Subhalo singularities strongly alter an otherwise fairly smooth distribution. Of course, this expected source of non-uniformity is best discarded. In a thin shell, there can only appear one subhalo, or perhaps a few of them. To avoid taking them into account in the computation of entropic coefficients, we can just remove a few of the most populated cells of every shell. This hardly alters the overall smoothness properties of the distribution in the shell but avoids subhalo singularities. We choose to remove the four most populated cells of every shell, reducing M to 60. Therefore, the entropic coefficients are given by

$$\frac{S_q(\{n_i\}_{i=1}^{60})}{\log_2 60} = \frac{S_q}{5.907}.$$

This simple operation reduces substantially the disturbing effects of subhalos.

Our complete procedure consists of splitting a halo in successive shells with 1024 particles each, in an onion-like structure, and computing a number of entropic coefficients for each shell, up to values of the radius such that the coefficients stabilize (if it so happens). The $q \geq 1$ coefficients must always decrease outwards. Assuming that the $q = 0$ Rényi dimension of the cosmic web is $D_0 = 3$, then the $q = 0$ entropic coefficient must be always close to one and the $q > 0$ coefficients must decrease outwards. Conversely, the $q < 0$ coefficients should increase outwards. For sufficiently large radii, all the coefficients must approach the

ones that correspond to the cosmic web. The variation of entropic coefficients with radius must display a gradual transition from smoothness to graininess (except for the local effects of subhalos). This transition is similar to the one found by Zemp et al [40].

In the next section, we consider the specific contribution of triaxiality as a smooth source of inequality of counts-in-cells.

2.3 Graininess versus triaxiality

The density in a spherical shell of a triaxial halo is not uniform, so the entropic coefficients can deviate from one even in the absence of real graininess. If the mass resolution of an N -body simulation halo were such that we could have a very large number of particles per shell, we could easily differentiate triaxiality from real graininess by substantially increasing the number of cells, M , which would make irrelevant any smooth variation of density, in particular, variations due to triaxiality. Indeed, by increasing M , we would be approaching the computation of Rényi dimensions, which are unaffected by any smooth variation of density. However, with only 1024 particles per shell and $M = 64$, we need to estimate the effect of triaxiality.

To see how anisotropy due to triaxiality but not to graininess reflects on the entropic coefficients computed with 1024 particles in 64 cells, we calculate these coefficients for a smooth distribution with considerable triaxiality, namely, a density with a deformed power-law radial profile: the density with profile r^{-2} subjected to an affine transformation to obtain axis ratios 2/3 and 1/3. Our smoothness measuring procedure, applied to 1024 points in a 0.4%-thick shell, yields coefficients 1, 0.965, 0.940, for $q = 0, 1, 2$, respectively. The last two coefficients differ significantly from one, yet they are close to one.² However, there are many Bolshoi halos with ratios of minor to major axis smaller than 1/3; and, in fact, there are even large halos with ratios close to 1/10. To prevent errors in the computation of entropic coefficients due to the effect of triaxiality combined with insufficient mass resolution, we may select quasi-spherical halos (with ratios of minor to major axis close to one). At any rate, it is worthwhile to examine some strongly triaxial halos for a comparison.

3 Smoothness of halos in N -body simulations

Now we analyze the smoothness of halos in the Bolshoi and VL2 simulations, with the procedure described above. We first summarize the characteristics of these simulations. Furthermore, since the multifractal properties of the cosmic web play a role in our arguments, we also provide the results of a multifractal analysis of the Bolshoi simulation, carried out as explained in appendix A (which is based on the techniques employed in [31] and, especially, in [33]).

3.1 Bolshoi and Via Lactea II simulations

The Bolshoi Λ CDM simulation is described by Klypin et al [36]. Here we quote its most relevant parameters. The simulation assumes cosmological parameters $\Omega_\Lambda = 0.73$, $\Omega_M = 0.27$, $\Omega_{\text{bar}} = 0.0469$, Hubble parameter $h = 0.70$, and initial spectral index $n = 0.95$. The edge length of the (comoving) simulation box is $250 h^{-1}$ Mpc and the number of particles $N = 2048^3$, which amounts to a mass resolution of $1.35 \cdot 10^8 h^{-1} M_\odot$ per particle and a discretization

²The $q = 0$ coefficient is smaller than 1 if one cell, at least, is empty (this coefficient is related to the void probability function [32]). But, if there are few empty cells, the difference is negligible.

length of $0.122 h^{-1}$ Mpc. The (Plummer) softening length is $1 h^{-1}$ kpc (physical, that is, not comoving). Our statistical analysis only requires the present time $z = 0$ snapshot and the corresponding list of halos, both obtained from the MultiDark database [37]. Naturally, we are interested in the bound-density-maxima (BDM) halos rather than in the friends-of-friends (FOF) halos (like in [36], where there is information about the latter as well).

The VL2 simulation [41] focuses on the formation of a single, Milky-Way size CDM halo, using the method of refinement. This simulation assumes cosmological parameters $\Omega_{\Lambda} = 0.76$, $\Omega_{\text{M}} = 0.24$, Hubble parameter $h = 0.73$, and initial spectral index $n = 0.95$. The edge length of the (comoving) simulation box is $40 h^{-1}$ Mpc. The halo is refined with more than 10^9 high-resolution particles, achieving a resolution of $4098 M_{\odot}$ per particle. The softening length is 40 pc (physical after $z = 9$).

3.2 Multifractal analysis of the Bolshoi simulation

The multifractal analysis of the Bolshoi simulation is carried out using the counts-in-cells method described in detail in appendix A. In the multifractal analysis of an N -body simulation by counts-in-cells, there are two scales that play a fundamental role: the homogeneity scale and the discretization length $N^{-1/3}$. The former is a physical scale, produced by the evolution of gravitational clustering, whereas the latter is intrinsic and indicates the scale at which the discretization effects dominate, on average. The multifractal cosmic-web structure must appear between those two scales. The homogeneity scale of the Bolshoi simulation, determined as explained in appendix A, is $l_0 = 15.6 h^{-1}$ Mpc, similar to the values found before in the GIF2 and Mare-Nostrum simulations [31, 33].³ Actually, the transition to homogeneity is not very sharp, beginning at a scale of about $8 h^{-1}$ Mpc and ending at about $30 h^{-1}$ Mpc. The discretization length, $N^{-1/3} = 2^{-11}$, is $0.12 h^{-1}$ Mpc.

The range between the discretization scale and the homogeneity scale in the Bolshoi simulation is four times larger than in the Mare-Nostrum simulation, as corresponds to the better resolution of the former. In the Mare-Nostrum simulation, the coarse multifractal spectra between scales 4 and $0.12 h^{-1}$ Mpc (a factor of 32) have been shown to coincide, in the ranges where α is defined [33]. In the Bolshoi simulation, we can proceed with the calculation of coarse multifractal spectra to lower scales, namely, down to $0.03 h^{-1}$ Mpc. The corresponding eight coarse multifractal spectra (corresponding to a scale factor of 128) are plotted in Fig. 2, on the left-hand side. They are similar to the ones of the Mare-Nostrum simulation and look like the typical multifractal spectrum of a self-similar multifractal [56]. The right-hand side of Fig. 2 shows the plot of the Rényi dimension D_q , computed at the scale $2.0 h^{-1}$ Mpc. This scale is in the middle of the interval of the three scales in Fig. 2 (left) that include the full multifractal spectrum, namely, that include the upper- α region, corresponding to voids.

For halos, we are going to use the $q = 1, 2$ entropic coefficients only. The Bolshoi cosmic-web multifractal analysis yields Rényi dimensions $D_1 = 2.46$ and $D_2 = 1.82$, which are similar to those obtained from other N -body simulations [31, 33]. If we divide D_1 and D_2 by three, resulting 0.82 and 0.61 , respectively, we have, approximately, the large- r values of the corresponding entropic coefficients of individual halos. However, the calculation of the D_q of a full N -body simulation involves an average and, on the other hand, the large-radius limit of the Rényi dimension of spherical shells can take substantially different values

³Remarkably, it is *exactly* the same value as in the Mare-Nostrum simulation [33]. This coincidence is due to our using cell sizes that are powers-of-two fractions of the simulation box edge, and to the box edge of the Bolshoi simulation being precisely one half of the box edge of the Mare-Nostrum simulation.

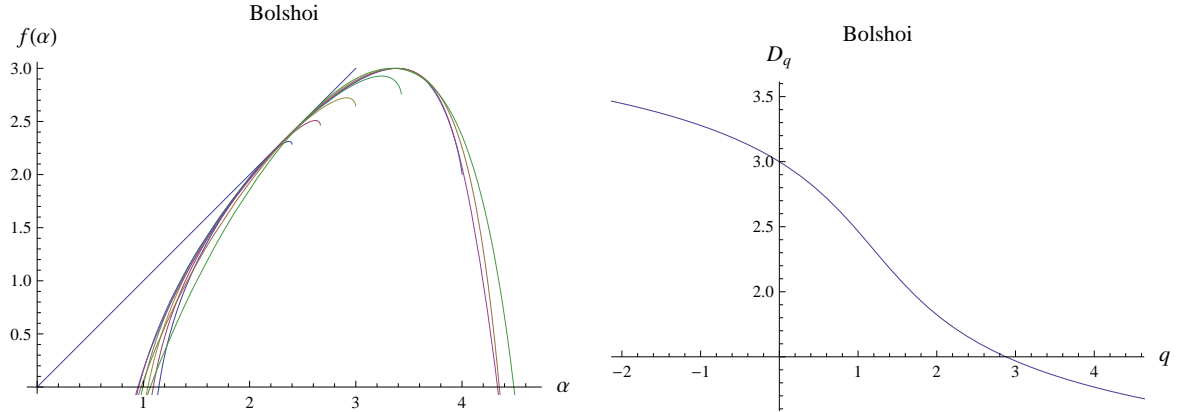


Figure 2. (Left) Coarse multifractal spectra of the Bolshoi simulation at relative scales $l = 2^{-13}, 2^{-12}, \dots, 2^{-6}$. (Right) Rényi dimensions at $l = 2^{-7}$.

for different halos. The Rényi dimension D_1 corresponds to the point in the multifractal spectrum such that $f(\alpha) = \alpha$, that is, to the so-called “measure’s concentrate” (the measure is the mass) [56] (see also appendix A). Since we can associate the region where the mass concentrates with the set of “typical” halos, we deduce that D_1 gives a better idea of the expected limit value of the corresponding entropic coefficient than D_2 does: indeed, $q = 2$ corresponds to especially concentrated halos, so the large-radius limit of the $q = 2$ Rényi coefficient of spherical shells of a “typical” halo should have a value larger than $D_2/3 = 0.61$.

Let us notice that two coarse multifractal spectra in Fig. 2 (left) correspond to scales smaller than the discretization length, which is $l = N^{-1/3} = 2^{-11}$. In consequence, those spectra only contain information on the smallest values of the local dimension α , that is to say, on the densest regions. The smallest scale, $l = 2^{-13}$, is really small, namely, $31 h^{-1}$ kpc, and the corresponding coarse multifractal spectrum hardly reaches the point that represents the concentrate of the mass. However, these coarse multifractal spectra, necessarily restricted to strong mass concentrations, seem to represent these concentrations fairly well.

3.3 Analysis of Bolshoi’s halos

The largest halo in the list of Bolshoi halos [37] has virial radius $r_{\text{vir}} = 2.14 h^{-1}$ Mpc, and there are 269 halos with $r_{\text{vir}} > 1 h^{-1}$ Mpc. The heaviest halos must be considered exceptional, if we take into account that there should be at least one normal halo per homogeneity volume. Let us quantify this concept of normality. If we take as the homogeneity volume a cube of $31.2 h^{-1}$ Mpc, which is the $1/512$ fraction of the simulation box volume, then about the 500 heaviest halos are exceptional (unless they have approximately the same mass, which is not the case). Let us recall that exceptional mass concentrations give rise to *negative* fractal dimensions in the multifractal analysis of N -body simulations, as explained in [33]. Therefore, we should exclude the top 500 halos, ordered by halo mass, say ($M_{\text{vir}} =$ mass of bound particles within r_{vir}). In fact, if we require negligible triaxiality, for example, a ratio of minor to major axis larger than 0.85, the largest compliant halo ranks 481th (in order of M_{vir}). This halo has $r_{\text{vir}} = 0.886 h^{-1}$ Mpc and $M_{\text{vir}} = 7.47 \cdot 10^{13} h^{-1} M_{\odot}$, and it is the heaviest halo that we analyze. We have analyzed a number of halos, calculating entropic coefficients for them, but we select for illustration only four: the heaviest halo and other three smaller quasi-spherical halos, with axis ratios larger than 0.9, which are distinct halos (not

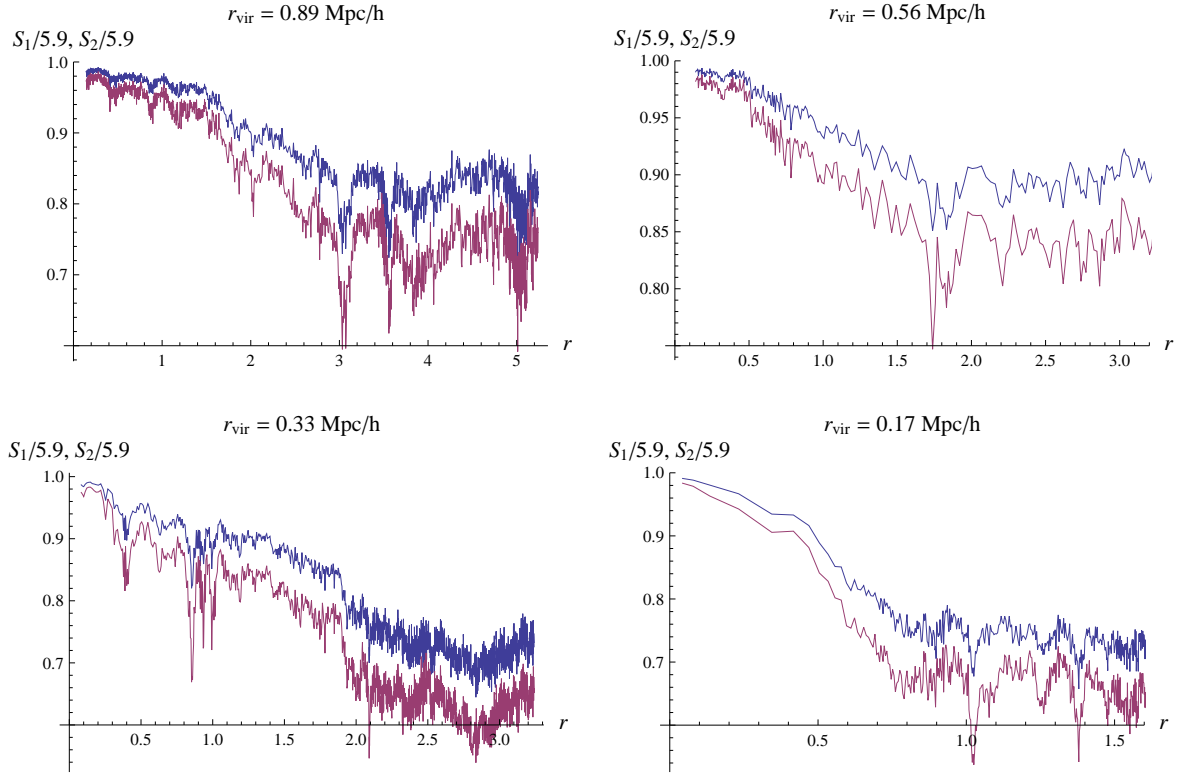


Figure 3. Smoothness, measured by entropic coefficients, versus radius (h^{-1} Mpc), in four quasi-spherical Bolshoi halos of decreasing virial radii. The upper (blue) lines correspond to the $q = 1$ entropic coefficients and the lower (red) lines correspond to the $q = 2$ coefficients.

subhalos), and spanning a considerable range of sizes. The transition from smoothness to graininess of each halo, as measured by the $q = 1$ and $q = 2$ entropic coefficients, is shown in Fig. 3. We can observe the progressive decrease of smoothness with radius, from values close to one (total smoothness) to asymptotic values that correspond to the multifractal cosmic-web structure. As expected, there are considerable fluctuations, due to subhalos, superposed on the decreasing trend (in spite of the elimination of the four most populated cells of every shell).

Remarkably, nothing special happens at the virial radius in regard to smoothness, in all the analyzed halos. Besides, there seems to be no proportionality or any correlation between the magnitudes of the virial radii and the “smoothness radii”. For example, the smoothness radius of the second halo in Fig. 3, with $r_{\text{vir}} = 0.56 h^{-1}$ Mpc and $M_{\text{vir}} = 1.97 \cdot 10^{13} h^{-1} M_{\odot}$, is smaller than the smoothness radius of the third one, with $r_{\text{vir}} = 0.33 h^{-1}$ Mpc and $M_{\text{vir}} = 3.01 \cdot 10^{12} h^{-1} M_{\odot}$. Furthermore, the second halo has higher values of the asymptotic entropic coefficients than the third one. All this suggests that the mass concentration is stronger in the third halo than in the second halo, in spite of the fact that the third halo has smaller virial radius and virial mass than the second one. If we measure the strength with the (coarse) local dimension [30, 31], namely,

$$\alpha = \frac{\log(M/M_0)}{\log(l/l_0)},$$

where M is the mass concentrated in a volume of diameter l and the values with subscript 0

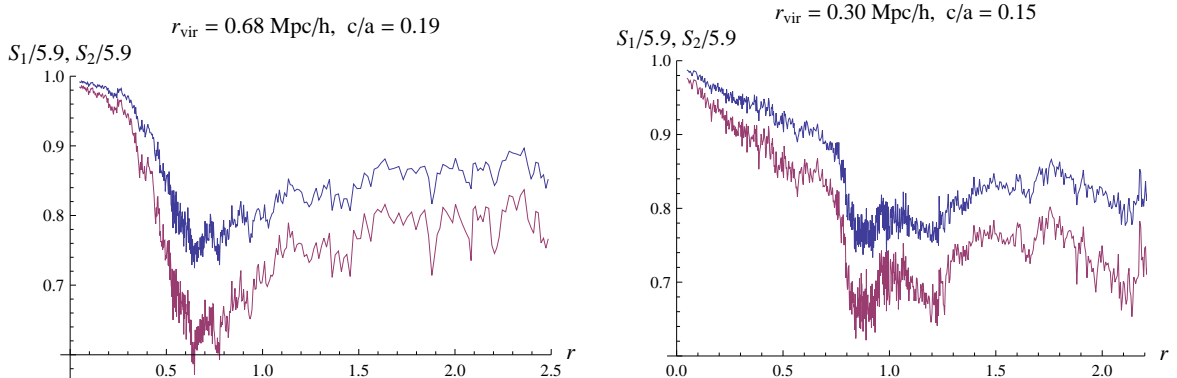


Figure 4. Smoothness of two triaxial Bolshoi halos with small ratios of minor to major axes, namely, $c/a < 0.2$.

correspond to homogeneity (with $l_0 = 31.2 h^{-1}$ Mpc), and we take as l twice the smoothness radius, then we obtain for the second halo $\alpha = 1.6$ and for the third one $\alpha = 1.4$. The latter indicates greater strength (let us recall that $\alpha \geq 0$, with 0 corresponding to the maximum strength).

Finally, we consider strongly triaxial halos, to determine the effect of the associated smooth but strong variation of density inside spherical shells. We have analyzed a number of them and we find no essential differences; namely, the overall pattern of variation of entropic coefficients is as shown in Fig. 3. However, the combined effect of triaxiality and insufficient mass resolution may give rise to dips at intermediate values of r in the plots of entropic coefficients, as shown in Fig. 4. It is natural that the intermediate scales, where triaxiality is fully developed and is the main anisotropic feature, are most affected. Let us notice again that any effect of triaxiality on the entropic coefficients should vanish with increasing mass resolution.

3.4 Analysis of the Via Lactea II halo

The analysis of graininess in the VL2 halo made by Zemp et al [40], employing the Gini coefficient and subhalo and void frequencies, shows that graininess steadily increases with radius. The Gini coefficient increases steadily from small values at small radii to $G = 0.3828$ at $r = 200$ kpc and to $G = 0.6193$ at $r = 400$ kpc (notice that the 200 background density radius is $r_{200b} = 402.1$ kpc). The conclusion is that the outskirts of dark matter halos have a clumpy structure [40]. Zemp et al do not specify what “the outskirts” are, but they surely mean the regions with $r \gtrsim 400$ kpc.

For our entropic analysis, we use the random subset of 100000 dark matter particles at redshift $z = 0$ within $r = 800$ kpc available at the VL project web-page [57]. The use of this subset might seem to reduce the resolution of the halo, but the random selection of a subset of particles at $z = 0$ is independent of the dynamics, which corresponds to the full set of particles. Nevertheless, the statistical errors of smoothness measures are larger in the reduced set of particles than in the full set. At any rate, 100000 particles are sufficient for our purposes, because this number is larger than the number of particles available for the smaller above-analyzed Bolshoi halos; so we expect that the values of the entropic coefficients are accurate. Of course, the Gini coefficients obtained with 100000 particles are not directly comparable with the ones obtained with the full set of particles by Zemp et al [40] (our

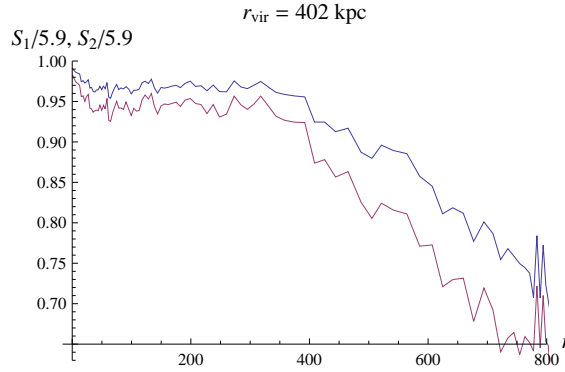


Figure 5. Decrease of smoothness ($q = 1, 2$ entropic coefficients) with increasing radius (in kpc) for the VL2 halo.

algorithm also computes the Gini coefficients, but they do not add any relevant information). The $q = 1$ and $q = 2$ entropic coefficients shown in Fig. 5 confirm Zemp et al’s results and give more information.

One remarkable feature of the plot of entropic coefficients (Fig. 5) is that these coefficients start decreasing in the first few kiloparsecs but thence stay nearly constant up to $r = 300$ kpc. This indicates that the distribution of particles is rather smooth, on average, for small radii and starts becoming grainy not far from r_{200b} . Zemp et al’s quantifiers, especially, the Gini coefficient, show it as well (see Table 1 in [40]). However, a detailed study of the VL2 distribution [41] shows that the inner density profile is “cuspy” (singular) and there are many subhalos close to the center. In fact, Diemand et al [41] write in the abstract: “We find hundreds of very concentrated dark matter clumps surviving near the solar circle, ... The simulation reveals the fractal nature of dark matter clustering.”

Finally, let us notice that, once that the decrease of smoothness begins in Fig. 5, it continues, and the coefficients do not seem to stabilize, although there is a slight indication that they may do so at the end of the plot. In any event, we have to take into account that the radius range in Fig. 5 is considerably smaller than in the plots of Fig. 3 and it is natural that the convergence to the cosmic web take place at larger radius.

4 N -body discreteness and smoothness of halos

The smoothness of the dark matter distribution in N -body simulations is presumably due to the combined effects of the diffusion by close encounters and of the softening of strong mass concentrations. Therefore, the smoothness of halos depends on both the discreteness parameters, namely, N (or the discretization length), and the softening length ϵ . The optimal choice of softening is a debated issue [43–46, 58, 59]. This problem can be formulated as follows: Given a bound gravitational structure of linear size R , for example, a dark matter halo represented by a set of N particles, the optimal softening length ϵ has to be determined in terms of N and R . There are several criteria to do it. The deduced dependence of the softening length ϵ on N and R goes from $\epsilon \sim RN^{-1}$, with the classic criterion of avoiding close encounters [60], to $\epsilon \sim RN^{-1/3}$, that is, a softening length of the order of the discretization length. The latter is certainly the safest choice [43–46]. Writing $\epsilon \sim RN^{-\beta}$, one has $1/3 \leq \beta \leq 1$. A sophisticated statistical criterion, based on the mean integrated square error (MISE) of the gravitational force, yields values of β that are in the range $0.2 \leq \beta \leq 0.44$

[58, 59], about the value $1/3$. The usual choice, $\epsilon \sim RN^{-1/2}$ [15, 42], does not guarantee small errors in halo centers [59].

One thing to notice in all these relations is that ϵ is proportional to R . This is imposed by dimensional analysis, but only in the case of dealing with an *isolated* set of N bound particles. In contrast, in cosmological N -body simulations, N is the total number of particles in the simulation box, which has nothing to do with the number of particles in one halo. In other words, we have another length parameter, namely, the size of the simulation box L , so ϵ does not have to be proportional to R . Assuming that the existence of individual halos bears no relation to the size of the simulation box and, hence, to the total number of particles N , it is better to express the softening length in terms of local quantities, namely, the discretization length, $\ell = LN^{-1/3}$, and the typical halo size, R . Now, dimensional analysis imposes no restrictions on the function $\epsilon(\ell, R)$. Of course, we are also assuming that the range of halo sizes is bounded and not too large, but this is the basic tenet of halo models [11]. Naturally, before thinking of a range of halo sizes, it is necessary to know how to define the size of a given halo. It is normal to choose the virial radius, derived through the spherical collapse model, but here we consider more reasonable to resort to the smoothness properties. In conclusion, a reasonable value of R for a given simulation should be some average of the smoothness size of normal halos (non-exceptional halos, in the sense discussed at the beginning of Sect. 3.3).

Since both the discreteness parameters ℓ and ϵ are fixed once and for all before starting the N -body simulation, whereas the sizes of halos belong to the result of the simulation, it is preferable to write the relation among the three quantities as $R(\ell, \epsilon)$. Ideally, this function would be weakly dependent on the variables ℓ and ϵ , so these parameters would have little influence on the size of halos, and the value of R could be ascribed to the initial conditions. In fact, there are evidences that point to a substantial influence of N -body discreteness [35].

In this regard, it would be very interesting to determine the *separate* influences of ℓ and ϵ on R . While a finite ℓ (a finite N) introduces corrections to the mean-field Vlasov-Poisson dynamics, partially remedied by the gravity softening, this softening also perturbs the Vlasov-Poisson dynamics. Joyce et al [46] discuss the separate role of both parameters and point out that the rigorous Vlasov-Poisson limit, $\ell \rightarrow 0$, is to be taken at *fixed* finite ϵ , resulting in a smoothed version of the Vlasov-Poisson equations. One may ask what $\lim_{\ell \rightarrow 0} R(\ell, \epsilon)$ is. To answer this question, dimensional analysis is again helpful, and $\lim_{\ell \rightarrow 0} R(\ell, \epsilon) \sim \epsilon$. This is natural, because, without discretization, the softening on a scale ϵ should produce smoothing on the same scale. In other words, if halo sizes are determined by smoothness, these sizes must be of the order of ϵ . Therefore, the subsequent $\epsilon \rightarrow 0$ limit that leads to the actual Vlasov-Poisson equations makes halo sizes vanish. Simultaneously, the number density of halos diverges. As suggested by Diemand et al [41]: “at infinite resolution one would find a long nested series of halos within halos within halos etc.” The simultaneous halo size vanishing and number-density diverging imply that the relevant solutions of the Vlasov-Poisson equations are *fully* singular, that is, contain non-isolated singularities, as corresponds to a multifractal cosmic web structure that is present on ever decreasing scales. Of course, the limit $\ell \rightarrow 0$ at *fixed* finite ϵ or, in other words, the domain of discreteness parameters such that $\epsilon \gg \ell$, is *not* studied by cosmological N -body simulations.

However, information on the domain $\epsilon \gg \ell$ is provided by the adhesion model [2–4, 8–10, 61]. In the adhesion model with finite viscosity ν , the cosmic-web sheets, filaments and nodes are not singular but have widths proportional to ν , which plays a regularizing role, like ϵ does in the Vlasov-Poisson equations. Since the adhesion model is analytically soluble in the limit $\nu \rightarrow 0$, the exact form of the distribution in this limit is known. In particular,

the solutions of the adhesion model corresponding to cosmological initial conditions contain, in the limit $\nu \rightarrow 0$, dense sets of singular mass concentrations of the three types: sheets, filaments and nodes [19]. By a set being “dense” is meant that any volume, however small, intersects the set. Remarkably, the formation of dense sets of singular mass concentrations is independent of the exact type of initial power spectrum of fluctuations and is due just to the bottom-up structure formation characteristic of CDM. If we associate the halo centers of the regularized Vlasov-Poisson equations with the nodes of the adhesion model, we deduce that, when the regularization is removed, halo sizes vanish and these zero-size “halos” become so prevalent that any volume contains an infinite number of them.

5 Summary and conclusions

To summarize, our analysis of the smoothness or, alternately, the graininess of halos is based on the application of robust entropic measures related to statistical measures of inequality that are employed in economy. The entropic coefficients that we have defined, being also related to Rényi dimensions, can actually measure properties of a continuous distribution of matter, unlike, for example, the Gini coefficient, employed by Zemp et al [40], which does not have a continuum limit. The entropic coefficients of spherical shells centered on a halo are well suited to describe the transition, as the shell radius grows, from smoothness or mild anisotropy to the graininess or strong anisotropy characteristic of a cosmic web structure. The entropic coefficients of a shell are calculated by employing counts-in-cells. We find it appropriate to use shells containing 1024 particles and use, for each shell, a 8×8 mesh on the unit square of cylindrical equal-area coordinates.

The would-be uniform distribution in an inner spherical shell of a halo is altered by two factors: halo shape, namely, halo triaxiality, and the possible intersection of the shell with subhalos. Both factors produce a varying density but do not really produce non-smoothness, except if the shell intersects singular subhalo centers. However, given that we have a limited number of particles per shell (chosen as 1024), the statistical estimation of entropic coefficients is subject to errors coming from both smooth and non-smooth sources of anisotropy, which are not easily distinguishable. To prevent anisotropy due to triaxiality, we may select quasi-spherical halos, but triaxiality only produces trivial modifications. At any rate, the worst source of anisotropy is the intersection with subhalo centers. We mitigate this effect by removing the four most populated cells of any shell (out of the total 64 cells). However, we find that the entropic coefficients fluctuate considerably, namely, they undergo frequent dips due to subhalos. Nevertheless, an average descending pattern is always clearly discernible.

We have analyzed several halos from the Bolshoi N -body simulation and, also, the Via Lactea II halo. We find, like Zemp et al, a progressive and essentially monotonic growth of graininess or anisotropy with growing radius and, furthermore, we observe, in every halo, that the growth of graininess stops at some radius and the amount of graininess stabilizes. The radius at which the limit graininess or anisotropy is attained marks the end of the smooth halo and the beginning of the cosmic web structure. Indeed, the limit values of the entropic coefficients agree with the Rényi dimensions of the cosmic web, which are computed independently. We find no proportionality or any other definite correlation between the smoothness radii and the virial radii of the analyzed halos, although there is a global trend of diminishing smoothness radii with virial radii. Besides, the smoothness radius normally is considerably larger than the virial radius. We propose that the smoothness radius gives an alternative measure of halo size that may be more convenient in some regards. Of course,

one must not necessarily conclude that smoothness is independent of dynamical relaxation to stable states (“virialization”) but just that the virial radius may not be an adequate measure of a stable state and also that relaxation may be influenced by N -body discreteness effects.

In fact, the smoothness of halos in N -body simulations can be mainly due to discreteness effects, as indicated by our qualitative analysis. A quantitative analysis of the effects of N -body discreteness demands a deeper understanding of the influence of the discreteness parameters or, in other words, of the nature of the function $R(\ell, \epsilon)$ that describes the size of halos in terms of the fundamental discreteness parameters, namely, the discretization length ℓ and the softening length ϵ . Nevertheless, we argue that the removal of these parameters in a physically meaningful way may lead to the vanishing of halo sizes, while the halo number density diverges.

References

- [1] Ya.B. Zeldovich, *Gravitational instability: An approximate theory for large density perturbations*, *Astron. & Astrophys.* **5** (1970) 84–89.
- [2] S.N. Gurbatov and A.I. Saichev, *Probability Distribution and Spectra of Potential Turbulence*, *Radiophys. Quant. Electr.* **27** (1984) 303–313.
- [3] S.F. Shandarin and Ya.B. Zel’dovich, *The large-scale structure of the universe: Turbulence, intermittency, structures in a self-gravitating medium*, *Rev. Mod. Phys.* **61** (1989) 185–220.
- [4] S.N. Gurbatov, A.I. Saichev and S.F. Shandarin, *Large-scale structure of the Universe. The Zeldovich approximation and the adhesion model*, *Phys. Usp.* **55** (2012) 223–249.
- [5] J. Einasto, M. Jõeveer and E. Saar, *Structure of superclusters and supercluster formation*, *MNRAS* **193** (1980) 353–375.
- [6] Ya.B. Zeldovich, J. Einasto and S.F. Shandarin, *Giant Voids in the Universe*, *Nature* **300** (1982) 407–413.
- [7] M.J. Geller and J.P. Huchra, *Mapping the Universe*, *Science* **246** (1989) 897–903.
- [8] L. Kofman, D. Pogosyan and S.F. Shandarin, *Structure of the universe in the two-dimensional model of adhesion*, *MNRAS* **242** (1990) 200–208.
- [9] D. H. Weinberg and J. E. Gunn, *Large-scale Structure and the Adhesion Approximation*, *MNRAS* **247** (1990) 260–286.
- [10] L. Kofman, D. Pogosyan, S.F. Shandarin and A.L. Melott, *Coherent structures in the universe and the adhesion model*, *The Astrophysical Journal* **393** (1992) 437–449.
- [11] A. Cooray and R. Sheth, *Halo models of large scale structure*, *Phys. Rep.* **372** (2002) 1–129.
- [12] H.J. Mo and S.D.M. White, *An analytic model for the spatial clustering of dark matter haloes*, *MNRAS* **282** (1996) 347–361.
- [13] P. Catelan, S. Matarrese and C. Porciani, *On the Spatial Distribution of Dark Matter Halos*, *Astrophys. J.* **502** (1998) L1–L4.
- [14] R.K. Sheth, and G. Tormen, *Large-scale bias and the peak background split*, *MNRAS* **308** (1999) 119–126.
- [15] C. Power et al, *The inner structure of CDM haloes - I. A numerical convergence study*, *MNRAS* **338** (2003) 14–34.
- [16] E. Hayashi et al, *The inner structure of CDM haloes - II. Halo mass profiles and low surface brightness galaxy rotation curves*, *MNRAS* **355** (2004) 794–812.

- [17] J.F. Navarro et al, *The inner structure of CDM haloes - III. Universality and asymptotic slopes*, *MNRAS* **349** (2004) 1039–1051.
- [18] B.B. Mandelbrot, *The fractal geometry of nature* (rev. ed. of: *Fractals*, 1977), W.H. Freeman and Company (1983).
- [19] M. Vergassola, B. Dubrulle, U. Frisch and A. Noullez, *Burgers’ equation, Devil’s staircases and the mass distribution for large-scale structures*, *Astron. & Astrophys.* **289** (1994) 325–356.
- [20] J. Gaite, *A non-perturbative Kolmogorov turbulence approach to the cosmic web structure*, *Europhys. Lett.* **98** (2012) 49002.
- [21] G. Rigopoulos, *The adhesion model as a field theory for cosmological clustering*, *JCAP* **1** (2015) 014.
- [22] J.P. Bouchaud, M. Mézard and G. Parisi, *Scaling and intermittency in Burgers turbulence*, *Physical Review E* **52** (1995) 3656–3674.
- [23] L. Pietronero, *The fractal structure of the universe: Correlations of galaxies and clusters and the average mass density*, *Physica A* **144** (1987) 257–284.
- [24] B.J. Jones, V. Martínez, E. Saar and J. Einasto, *Multifractal description of the large-scale structure of the universe*, *Astrophys. J.* **332** (1988) L1–L5.
- [25] R. Balian and R. Schaeffer, *Galaxies: Fractal dimensions, counts in cells, and correlations*, *Astrophys. J.* **335** (1988) L43–L46.
- [26] B.J. Jones, V. Martínez, E. Saar and V. Trimble, *Scaling laws in the distribution of galaxies*, *Rev. Mod. Phys.* **76** (2004) 1211–1266.
- [27] R. Valdarnini, S. Borgani and A. Provenzale, *Multifractal properties of cosmological N-body simulations*, *Astrophys. J.* **394** (1992) 422–441.
- [28] S. Colombi, F.R. Bouchet and R. Schaeffer, *Multifractal analysis of a cold dark matter universe*, *Astron. & Astrophys.* **263** (1992) 1.
- [29] G. Yepes, R. Domínguez-Tenreiro and H.P.M. Couchman, *The scaling analysis as a tool to compare N-body simulations with observations — Application to a low-bias cold dark matter model*, *Astrophys. J.* **401** (1992) 40–48.
- [30] J. Gaite, *The fractal distribution of haloes*, *Europhys. Lett.* **71** (2005) 332–338.
- [31] J. Gaite, *Halos and voids in a multifractal model of cosmic structure*, *Astrophys. J.* **658** (2007) 11–24.
- [32] J. Gaite, *Statistics and geometry of cosmic voids*, *JCAP* **11** (2009) 004.
- [33] J. Gaite, *Fractal analysis of the dark matter and gas distributions in the Mare-Nostrum universe*, *JCAP* **3** (2010) 006.
- [34] C.A. Chacón-Cardona and R.A. Casas-Miranda, *Millennium simulation dark matter haloes: multifractal and lacunarity analysis and the transition to homogeneity*, *MNRAS* **427** (2012) 2613–2624.
- [35] J. Gaite, *Halo Models of Large Scale Structure and Reliability of Cosmological N-Body Simulations*, *Galaxies* **1** (2013) 31–43.
- [36] A.A. Klypin, S. Trujillo-Gomez and J. Primack, *Dark Matter Halos in the Standard Cosmological Model: Results from the Bolshoi Simulation*, *Astrophys. J.* **740** (2011) 102.
- [37] K. Riebe et al, *The MultiDark Database: Release of the Bolshoi and MultiDark Cosmological Simulations* [[arXiv:1109.0003](https://arxiv.org/abs/1109.0003)].
- [38] A. Knebe et al, *Structure finding in cosmological simulations: the state of affairs*, *MNRAS* **435** (2013) 1618–1658.

- [39] D.H. Weinberg et al, *Cold dark matter: controversies on small scales* [[arXiv:1306.0913](https://arxiv.org/abs/1306.0913)].
- [40] M. Zemp et al, *The graininess of dark matter haloes*, *MNRAS* **394** (2009) 641–659.
- [41] J. Diemand et al, *Clumps and streams in the local dark matter distribution*, *Nature* **454** (2008) 735–738.
- [42] W. Dehnen and J.I. Read, *N-body simulations of gravitational dynamics*, *Eur. Phys. J. Plus* **126** (2011) 55:1–55:28.
- [43] B. Kuhlman, A.L. Melott and S.F. Shandarin, *A Test of the Particle Paradigm in N-Body Simulations*, *Astrophys. J.* **470** (1996) L41.
- [44] R.J. Splinter, A.L. Melott, S.F. Shandarin and Y. Suto, *Fundamental Discreteness Limitations of Cosmological N-Body Clustering Simulations*, *Astrophys. J.* **497** (1998) 38–61.
- [45] A.B. Romeo, O. Agertz, B. Moore and J. Stadel, *Discreteness Effects in CDM Simulations: A Wavelet-Statistical View*, *Astrophys. J.* **686** (2008) 1–12.
- [46] M. Joyce, B. Marcos and T. Baertschiger, *Towards quantitative control on discreteness error in the non-linear regime of cosmological N-body simulations*, *MNRAS* **394** (2009) 751–773.
- [47] S.F. Shandarin, *The multi-stream flows and the dynamics of the cosmic web*, *JCAP* **15** (2011) 005.
- [48] T. Abel, O. Hahn and Kaehler, *Tracing the dark matter sheet in phase space*, *MNRAS* **427** (2012) 61–76.
- [49] M. Neyrinck, *Origami constraints on the initial-conditions arrangement of dark-matter caustics and streams*, *MNRAS* **427** (2012) 494–501.
- [50] V. Sahni, B.S. Sathyaprakash and S.F. Shandarin, *Shapefinders: A New Shape Diagnostic for Large-Scale Structure*, *The Astrophysical Journal* **495** (1998) L5.
- [51] J.V. Sheth, V. Sahni, S.F. Shandarin and B.S. Sathyaprakash, *Measuring the geometry and topology of large-scale structure using SURFGEN: methodology and preliminary results*, *MNRAS* **343** (2003) 22–46.
- [52] R. van de Weygaert and W. Schaap, *The Cosmic Web: Geometric Analysis*, in *Data Analysis in Cosmology (Valencia)*, eds. V. Martínez, E. Saar, E. Martínez-Gonzalez, M.J. Pons-Bordería, *Lecture Notes in Physics*, vol. 665, Springer-Verlag (2009) 291–413.
- [53] E.W. Weisstein, *Cylindrical Equal-Area Projection*, from MathWorld — A Wolfram Web Resource [<http://mathworld.wolfram.com/CylindricalEqual-AreaProjection.html>].
- [54] A. Ullah and D.E.A. Giles (Eds.), *Handbook of Applied Economic Statistics*, CRC Press (1998).
- [55] A. Rényi, *Calcul des probabilités*, Dunod, Paris (1966).
- [56] K. Falconer, *Fractal Geometry (Second Edition)*, John Wiley and Sons, Chichester UK, (2003), Chapter 17.
- [57] J. Diemand et al, *The via lactea project* [<http://www.ics.uzh.ch/~diemand/vl>].
- [58] D. Merritt, *Optimal Smoothing for N-Body Codes*, *Astronom. J.* **111** (1996) 2462–2464.
- [59] Hu Zhan, *Optimal Softening for N-Body Halo Simulations*, *Astrophys. J.* **639** (2006) 617–620.
- [60] J. Binney and S. Tremaine, *Galactic Dynamics (Second Edition)*, Princeton University Press (2008), pg. 33.
- [61] T. Buchert and A. Domínguez, *Adhesive gravitational clustering*, *Astron. & Astrophys.* **438** (2005) 443–460.

A Appendix: multifractal analysis

Coarse multifractal analysis is appropriate, in general, for physical examples and the results of simulations [56]. For a distribution of particles, the mass (the “measure”) is discretized and the method comes down to an elaboration of the counts-in-cells statistics that is common in the analysis of N -body simulations.

Let us assume that a mesh of cells is placed in the sample region, that is, for our purposes, either the full simulation box or the unit square that corresponds to a spherical shell of a halo (Sect. 2.1). Fractional statistical moments are defined by counts in cells as

$$M_q = \sum_i \left(\frac{n_i}{N} \right)^q = \sum_{n>0} N(n) \left(\frac{n}{N} \right)^q, \quad (\text{A.1})$$

where the index i refers to non-empty cells, n_i is the number of particles in the cell i , $N = \sum_i n_i$ is the total number of particles, and $N(n)$ is the number of cells with n particles. The second expression involves a sum over cell populations that is more useful than the sum over individual cells when most cells are scarcely populated. M_0 is the number of non-empty cells and M_1 is normalized to 1.

In regular distributions, the mass (number of particles) contained in any cell must be proportional to the cell’s volume, v , for sufficiently small v . Therefore, $M_q \sim v^{q-1}$. This does not apply to singular distributions, but they can be such that their q -moments are non-trivial power laws of v in the $v \rightarrow 0$ limit. So one can define, for a singular distribution, the non-trivial exponents

$$\tau(q) = 3 \lim_{v \rightarrow 0} \frac{\log M_q}{\log v}, \quad q \in \mathbb{R}, \quad (\text{A.2})$$

provided that the limit exists. Such a distribution is called multifractal. Of course, the numerical evaluation of the limit in Eq. (A.2) is not feasible and one must be satisfied with finding a constant value of the quotient for sufficiently small v , that is, in a range of negative values of $\log v$ (a range of scales). In fact, the exponent is normally defined as the slope of the plot of $\log M_q$ versus $\log v$, and its value is found by numerically fitting that slope.

A multifractal is also characterized by its *local* dimensions. The local dimension α at the point \mathbf{x} expresses the asymptotic power-law form of the mass growth from that point outwards, $m(\mathbf{x}, r) \sim r^{\alpha(\mathbf{x})}$, and defines the “strength” of the corresponding singularity. Actually, singularities correspond to $\alpha < 3$, whereas points with $\alpha \geq 3$ are regular. Every set of points with a given local dimension α constitutes a fractal set with a dimension that depends on α , namely, $f(\alpha)$. In terms of $\tau(q)$, the spectrum of local dimensions is given by

$$\alpha(q) = \tau'(q), \quad q \in \mathbb{R}, \quad (\text{A.3})$$

and the spectrum of fractal dimensions $f(\alpha)$ is given by the Legendre transform

$$f(\alpha) = q \alpha - \tau(q). \quad (\text{A.4})$$

Self-similar multifractals have a typical spectrum of fractal dimensions that spans an interval $[\alpha_{\min}, \alpha_{\max}]$, is convex from above, and fulfills $f(\alpha) \leq \alpha$. Furthermore, the equality $f(\alpha) = \alpha$ is reached at one point, such that $q = 1$ in Eq. (A.4): note that Eq. (A.2) gives $\tau(1) = 0$. The corresponding set of singularities contains the bulk of the mass and is called the “mass concentrate.”

As said above, the convergence to the limit in Eq. (A.2) must take place in a range of small values of v . Naturally, v must be small in comparison with the homogeneity volume v_0 , which is the smallest volume such that the mass fluctuations in it are small and approximately Gaussian. Therefore, we define, for a given cell size v , the *coarse* exponent

$$\tau(q) = 3 \frac{\log(M_q/v_0^{q-1})}{\log(v/v_0)}. \quad (\text{A.5})$$

For cell sizes larger than v_0 , $M_q \sim v^{q-1}$ and $\tau(q) = 3(q-1)$. The coarse exponent τ depends on both v and v_0 , but it must depend mildly on the latter. Nevertheless, this dependence on v_0 is generally non-negligible: if one just sets v_0 to 1, that is to say, to the total volume, as often done, the coarse exponents may be so inaccurate that the multifractal scaling is spoiled. In other words, if v_0 is not included, the available range of v may not be long enough for us to obtain reliable values of the functions $\tau(q)$ and $f(\alpha)$. One can estimate v_0 as, for example, the coarse-graining scale such that the mass fluctuations are smaller than a given fraction, say, 10%.

As a complement to the multifractal spectrum $f(\alpha)$, it is useful to define the spectrum of Rényi dimensions

$$D_q = \frac{\tau(q)}{q-1}, \quad (\text{A.6})$$

because they have an information-theoretic meaning. Indeed, they are related to Rényi entropies [55]; namely, they express the power-law behavior of the Rényi entropies of the coarse distribution in the limit $v \rightarrow 0$:

$$D_q = \lim_{v \rightarrow 0} \frac{3 S_q(\{p_i\})}{-\log_2 v}.$$

Rényi entropies, in general, measure the lack of information or the uncertainty of a probability distribution. In the case of a discrete distribution of particles, they measure the uncertainty in the choice of q particles (when q is a positive integer). The dimension of the mass concentrate $\alpha_1 = f(\alpha_1) = D_1$ is also called the entropy dimension. D_0 coincides with the maximum value of $f(\alpha)$ and q with the box-counting dimension of the distribution's support, while $D_2 = \tau(2)$ is the correlation dimension. In the homogeneous regime, $\tau(q) = 3(q-1)$ and $D_q = 3$ for any q . In a uniform fractal (a *unifractal* or *monofractal*) D_q is also constant but smaller than three. In general, D_q is a non-increasing function of q .